Adv. Space Res. Vol.12, No.11, pp.(11)47–(11)54, 1992
Printed in Great Britain.

0273-1177/92 $15.00

PLASMA WAVE OBSERVATIONS AT NEPTUNE

D. A. Gurnett,* W. S. Kurth,* L. J. Granroth,* I. H. Cairns,*
W. M. Macek,*,** R. L. Poynter,*** S. L. Moses,† F. V. Coroniti,†
C. F. Kennel† and D. D. Barbosa‡

* *Department of Physics and Astronomy, University of Iowa, Iowa City, IA 52242, U.S.A.*
** *Space Research Centre, Polish Academy of Sciences, PL-01 237 Warsaw, Ordona 21, Poland*
*** *Jet Propulsion Laboratory, 4800 Oak Grove Drive, Pasadena, CA 91109, U.S.A.*
† *TRW Space and Technology Group, One Space Park, Redondo Beach, CA 90278, U.S.A.*
‡ *Institute of Geophysics and Planetary Physics, UCLA, Los Angeles, CA 90024, U.S.A.*

ABSTRACT

During the Voyager 2 flyby of Neptune, the plasma wave instrument detected many familiar phenomena. These include radio emissions, electron plasma oscillations in the solar wind upstream of the bow shock, electrostatic turbulence at the bow shock, electrostatic electron cyclotron waves and upper hybrid resonance (UHR) waves, whistler mode noise, and dust impacts. The radio emissions occur in a broad continuum-like spectrum extending from about 5 kHz to above 50 kHz, and are emitted in a disk-like beam along the magnetic equatorial plane. The radio emissions are believed to be generated by mode conversion from UHR waves at the magnetic equator. The inner magnetosphere has relatively low plasma wave intensities, generally less than 100 μV/m. At the ring plane crossing, many small micron-sized dust particles were detected striking the spacecraft. The maximum impact rate was about 280 impacts per second at the inbound ring plane crossing, and about 110 impacts per second at the outbound ring plane crossing. Most of the particles are concentrated in a dense disk, about one thousand km thick, near the equatorial plane. A broader, more tenuous distribution of dust also extends along the entire trajectory inside of 6 R_N including the northern polar region.

INTRODUCTION

On 25 August 1985 the Voyager 2 spacecraft flew by Neptune, thereby providing the first evidence that the planet has a magnetosphere and radiation belt. In this paper we review the results from the Voyager 2 plasma wave instrument. This instrument was designed to detect the electric field of plasma waves from 10 Hz to 56 kHz. For further details on the design and operation of this instrument see Scarf and Gurnett /1/. An initial report describing the plasma wave observations at Neptune was published by Gurnett et al. /2/. Several additional studies have also been completed /3,4,5,6/. Our objective here is to briefly review all of the results available up to the present time. To organize the presentation, the results are described more or less in the order in which the data were obtained, starting first with the upstream waves detected during the approach to Neptune, and ending with a discussion of the various phenomena observed in the inner regions of the magnetosphere.

UPSTREAM WAVES, BOW SHOCK, AND MAGNETOPAUSE

During the approach to Neptune the first evidence of upstream waves associated with the magnetosphere occurred at 1055 spacecraft event time (SCET) on 24 August 1989. At this time a weak burst of electron plasma oscillations was detected in the 562-Hz channel of the 16-channel spectrum analyzer. About an hour and a half later, at 1252 SCET, the plasma oscillations reappeared in the same channel, this time stronger (~100 μV/m) and more nearly continuous. These electron plasma oscillations are indicated in Figure 1, which shows the electric field intensities from the 16-channel spectrum analyzer for a 32-hour interval centered on closest approach. From previous encounters with planetary magnetospheres it is known that electron plasma oscillations are generated in the solar wind upstream of the planet by suprathermal electrons streaming outward from the bow shock. Since the electrons tend to move along the solar wind magnetic field lines, the presence of electron plasma oscillations indicates that the spacecraft was now on magnetic field lines that intersect the bow shock. Indeed, about an hour and three quarters later, at 1435 SCET, the spacecraft crossed the bow shock. The bow shock crossing was characterized by an abrupt broadband burst of noise in the 10-Hz to 178-Hz channels. The electric field noise associated with the shock crossing is indicated in Figure 1. The radial distance from the center of the planet at the time of the shock crossing was about 35.0 R_N. Further details and analyses of the electric field noise detected at the bow shock are given by Moses et al. /6/. After exiting the bow shock, the plasma wave electric field intensities dropped to undetectable levels as the spacecraft passed through the magnetosheath. The absence of detectable waves in the magnetosheath is typical of the outer planets. Although the magnetic field /7/ and plasma /8/ instruments detected a broad disordered crossing of the magnetopause from about 1800 to 1935 SCET, no indication of the magnetopause crossing was evident in the plasma wave data.

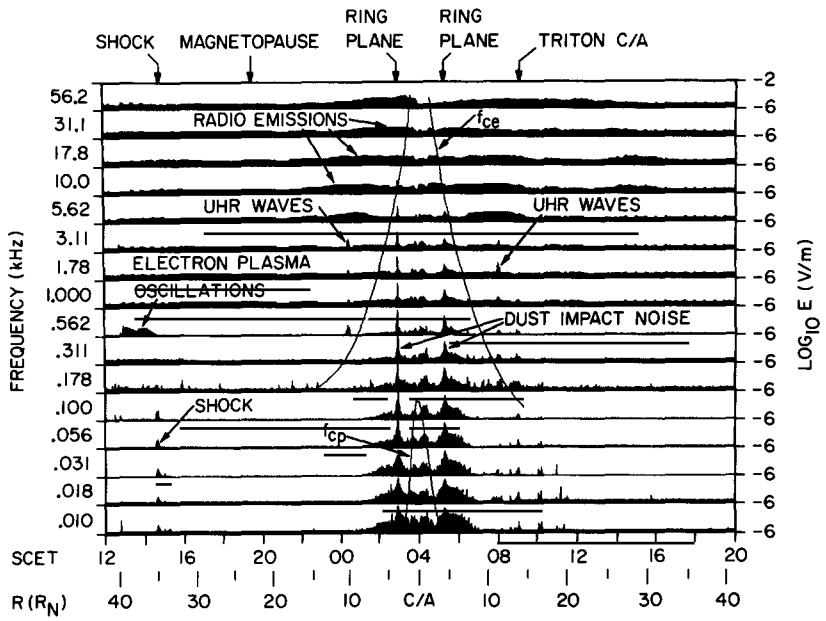

Fig. 1. A 16-channel plot of the electric field strengths detected by the Voyager plasma wave instrument during the flyby of Neptune.

RADIO EMISSIONS AND UPPER HYBRID WAVES

The plasma wave instrument first started to detect low-frequency (<100 kHz) radio emissions from Neptune's magnetosphere a few days before closest approach. However, the radio emissions were very weak and did not rise significantly above the instrument noise level until the spacecraft was well inside the magnetosphere. The low-frequency radio emissions can be seen in the 5.62- through 56.2-kHz channels in Figure 1. The upper-frequency range of the radio emissions extends well above 56.2 kHz, into the frequency range of the planetary radio astronomy instrument /9/. Wideband waveform measurements, which provide very high resolution spectrum measurements from 50 Hz to 12 kHz, show that the spectrum is smooth and continuous, very similar to continuum radiation in the Earth's magnetosphere /10/. For this reason we are calling this radio emission continuum radiation.

The intensity of the Neptunian continuum radiation generally increases with decreasing radial distance. However, as can be seen in Figure 1, the intensity drops to undetectable levels for a brief (~45 minute) period near closest approach (CA). The absence of continuum radiation near closest approach is most likely a propagation effect caused by high plasma densities encountered as the spacecraft passed through the ionosphere of Neptune. In addition to the radial distance dependence the continuum radiation also has a well-defined modulation at the same 16-hour planetary rotation period identified by the planetary radio astronomy experiment /9/. Two peaks occur in the intensity per rotation. This modulation pattern suggests that the radiation is beamed outward from the planet in a disk-like beam that rotates with the planetary magnetic field. Analysis of the timing of the two peaks /3/ shows that the tilt and phase of the radiation pattern are consistent with the tilt and phase of the offset-tilted-dipole (OTD) model of Neptune's magnetic field /7/. The plane of the radio emission beam is oriented along the magnetic equatorial plane, more-or-less as shown in Figure 2.

In the Earth's magnetosphere, as well as at several other planets, continuum radiation is believed to be produced by mode conversion from intense electrostatic waves generated near the magnetic equator /11/. It now appears that a similar process may be responsible for the generation of continuum radiation at Neptune. As the spacecraft passed through the magnetosphere, intense narrowband emissions were observed in the 3.11-kHz channel at 0025 SCET on the inbound leg, and again in the 1.78-kHz channel at 0800 SCET on the outbound leg. These emissions can be seen in Figure 3, which shows a spectrogram representation of the same data as in Figure 1, but over a shorter time interval to give better resolution of the inner regions of the magnetosphere. These emissions occur almost exactly at the magnetic equator, as determined from the OTD magnetic field model of Ness et al. /7/. Comparisons with the magnetic field /7/ and plasma /8/ data also show that the frequency of these emissions is very close to the upper hybrid resonance frequency, $f_{UHR} = \sqrt{f^2_{ce} + f^2_{pe}}$, where f_{ce} is the electron cyclotron frequency (f_{ce} = 28 B Hz, where B is the magnetic field in nT) and f_{pe} is the electron plasma frequency (f_{pe} = 9000 $\sqrt{N}$ Hz, where N is the electron density in cm^{-3}). At other planets UHR emissions of this type are often closely associated with bands of electrostatic waves that occur near half-integral harmonics, $(n + 1/2)f_{ce}$, of the electron cyclotron frequency. Weak emissions most likely associated with low half-integral

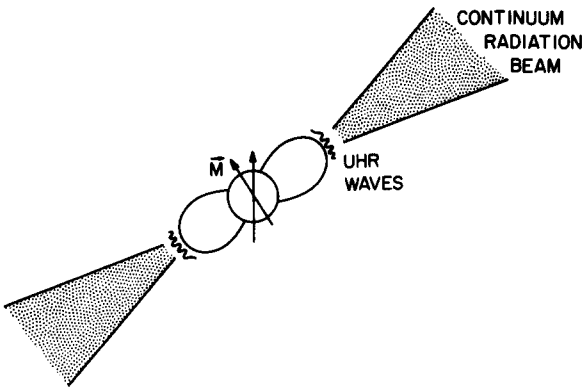

Fig. 2. A schematic representation of the generation of the low frequency (5 to 50 kHz) continuum radiation. This radiation is believed to be produced by mode conversion from electrostatic upper hybrid resonance (UHR) waves.

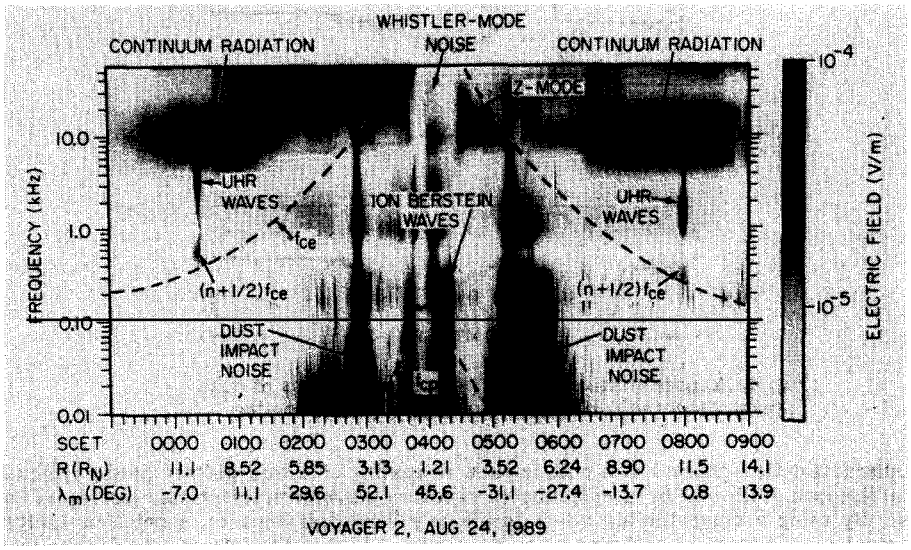

Fig. 3. A frequency-time spectrogram of the plasma wave electric field intensities at radial distances inside of about 15 R_N.

harmonics of f_{ce} can also be seen in Figure 3. For a further analysis of these waves see Barbosa et al. /4/. Figure 3 also shows that the UHR waves occur near and slightly below the lower cutoff of the continuum radiation. This situation is very similar to the relationship between UHR waves and continuum radiation in the Earth's magnetosphere, and strongly suggests that the continuum radiation is being generated by mode conversion from the UHR waves. The basic idea is illustrated in Figure 2, which shows the continuum radiation propagating outward from a region of intense UHR waves. Since the UHR frequency increases with decreasing radial distance (because of the B dependence), the radio emission is spread into a continuous distribution of frequencies. At any given radial distance the local UHR frequency defines the lower edge of the band of continuum radiation. The UHR waves are most likely driven by low energy electrons that are magnetically confined to the equatorial region of the magnetosphere.

DUST IMPACTS

Two ring plane crossings occurred during the Voyager 2 flyby of Neptune, the first on the inbound pass at 0253:02 SCET, and the second on the outbound pass at 0514:51 SCET. As can be seen from Figures 1 and 3, very high noise levels were observed by the plasma wave instrument at both ring plane crossings. This

noise is believed to be caused by many small micron-sized particles striking the spacecraft. The sensitivity of the plasma wave instrument to dust impacts was first discovered during the Voyager 2 ring plane crossing at Saturn /12/. When a small dust particle strikes the spacecraft at a high velocity the particle is instantly vaporized and heated to a high temperature. For velocities greater than a few km/s the temperature is so high that a substantial amount of the material is ionized. As the resulting plasma cloud expands outward from the impact site, some of the charge is collected by the antenna, thereby producing a voltage pulse in the receiver. Laboratory measurements show that the charge collected is proportional to the mass of the impacting particle. The amplitude of the voltage pulse detected by the instrument is therefore proportional to the mass of the particle.

Since Neptune was known to have a ring system, it was anticipated that dust impacts would be detected by the plasma wave instrument at the ring plane crossings. For this reason a series of 48-second wideband waveform frames were scheduled around the times of the ring plane crossings. These waveform measurements provided a nearly continuous sample of the antenna voltage at a rate of 28,800 samples per second, thereby allowing individual impacts to be detected and counted. Three representative voltage waveforms obtained during the inbound ring plane crossing are shown in Figure 4. These waveforms

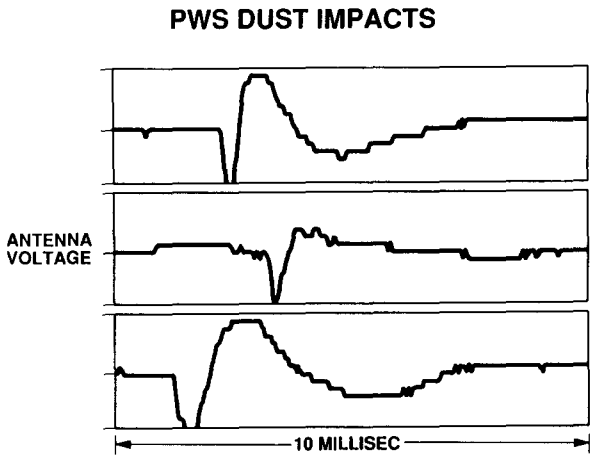

Fig. 4. Representative antenna voltage waveforms of dust impacts detected during the inbound ring plane crossing.

display the characteristic signature of a dust impact, consisting of a well-defined pulse, typically lasting about one millisecond, followed by a complicated recovery waveform sometimes lasting as long as 10 milliseconds. By using a computer algorithm to identify individual impacts, a detailed analysis of the impact rate can be performed for both ring plane crossings. A plot of the impact rate for the inbound ring plane crossing is shown in Figure 5 as a function of time and as a function of the distance Z from the equatorial plane (measured positive in the northward direction). As can be seen the impact rate rises steeply, reaches a maximum at 0253:19 ± 4s SCET, about 17 ± 4 seconds after the nominal equator crossing, and then declines. The radial distance at the time of maximum impact rate is 3.44 R_N. The 17-second delay corresponds to a northward offset of ΔZ = 155 km from the equatorial plane. The north-south thickness of the dust impact region (to the half intensity points) is about one thousand km.

On the outbound ring plane crossing the maximum impact rate occurred at 0516:07 ± 4s SCET, about 76 ± 4 seconds after the nominal equator crossing. The radial distance at the time of maximum impact rate was 4.26 R_N. The 76-second delay corresponds to a southward offset of ΔZ = -569 km from the equatorial plane. The north-south thickness of the dust impact region is several thousand km, substantially larger than on the inbound crossing. Although the main dust impact region is concentrated near the equatorial plane, the spectrum analyzer data display an impulsive spiky appearance over the entire region from 0150 to 0620 SCET, including the polar region. Although wideband waveform data is not available to confirm the origin of this impulsive noise, it seems most likely that the noise is caused by dust impacts. The impact rate over the polar region is estimated to be at least one impact every few seconds.

Although the impact rate can be determined with good accuracy, because of the uncertainties in the coupling process, it is very difficult to accurately estimate the size and mass of the particles. At the present time a detailed analysis of the size and mass distribution has not been carried out. However, since the waveform shapes and ratio of r.m.s. voltage to impact rate are very similar to the dust impacts observed at Saturn, most likely the dust particles are of similar mass. Various analyses /13,14/ indicate that the dust particles detected at Saturn have masses in the range from 10^{-12} to 10^{-9} gm, which corresponds to diameters in the range from 1 to 10 μm, assuming a density of about 1 gm/cm^3.

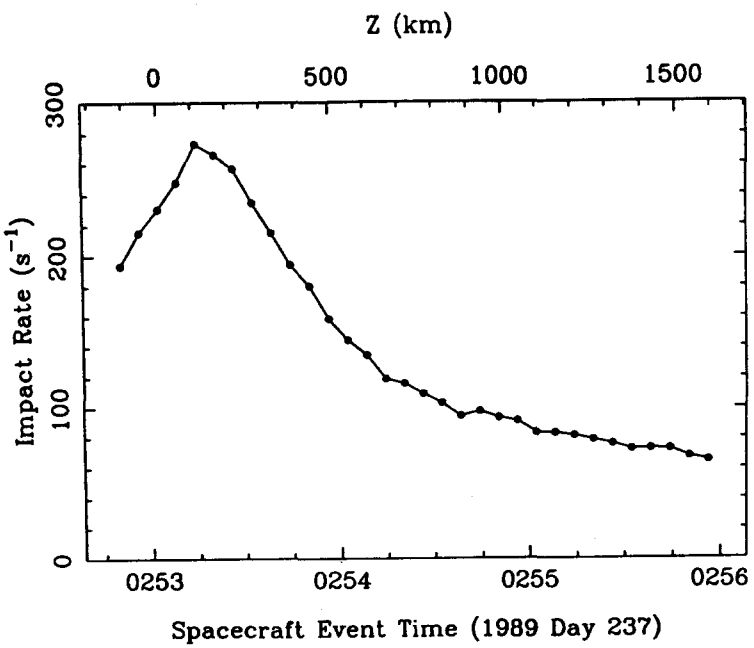

Fig. 5. The dust impact rate observed during the inbound ring plane crossing. Note that the peak impact rate is shifted slightly north of the equatorial plane (z = 0).

WHISTLERS

As is well known, whistlers are electromagnetic waves excited by lightning that propagate through the magnetosphere at frequencies below the electron cyclotron frequency and electron plasma frequency /15/. Because of the dispersive nature of the propagation in the magnetospheric plasma, the impulsive signal from a lightning flash is converted into a whistling tone, hence the term "whistler." At low frequencies the travel time obeys a relationship known as the Eckersley law /16/

$$t = D/\sqrt{f} \qquad (1)$$

where t is the travel time, f is the frequency, and D is a constant known as the dispersion. Because the magnetic field introduces an anisotropy in the plasma, whistlers tend to be guided along the magnetic field, often bouncing many times from one hemisphere to the other.

During the Voyager 2 pass through the inner regions of Neptune's magnetosphere, a total of 16 whistler-like signals were detected. These signals were all visually identified in high resolution frequency-time spectrograms of the wideband data. The location of the wideband frames is summarized in Figure 6, which shows the spacecraft trajectory in the region near closest approach. The solid black dots indicate wideband frames in which whistlers were observed. Each whistler is identified by a number. An example of a wideband spectrogram with a whistler is shown in Figure 7. This spectrogram shows whistler No. 4, which is one of the best events. The unmistakable characteristic of a whistler, consisting of a narrowband tone decreasing monotonically in frequency with increasing time, is clearly evident. Careful measurements /5/ show that the travel time as a function of frequency follows the Eckersley law, thereby providing strong evidence that the signals are generated by lightning in Neptune's atmosphere. The dispersions are very large, with all except one of the dispersions falling in the range from 24,330 to 29,209 sec $Hz^{-1/2}$. The one exception (whistler No. 1) has a dispersion of 45,462 sec $Hz^{-1/2}$. The frequencies range from 6.1 to 12.0 kHz. In several cases the upper limit, 12.0 kHz, is determined by the upper cutoff of the wideband receiver rather than by the actual frequency range of the signal. In all cases the signals are very weak, only slightly above the receiver noise level.

The dispersions of the whistlers observed at Neptune are very large, much larger than the typical dispersions of whistlers in the Earth's magnetosphere. The interpretation of the large dispersions is complicated by the great uncertainties that exist in the magnetic field configuration and plasma density distribution in the inner regions of Neptune's magnetosphere. It is relatively easy to show that for field-aligned propagation the dispersion is given by the following integral evaluated along the ray path

$$D = \frac{1}{2c} \int \frac{f_p}{\sqrt{f_c}} ds \qquad (2)$$

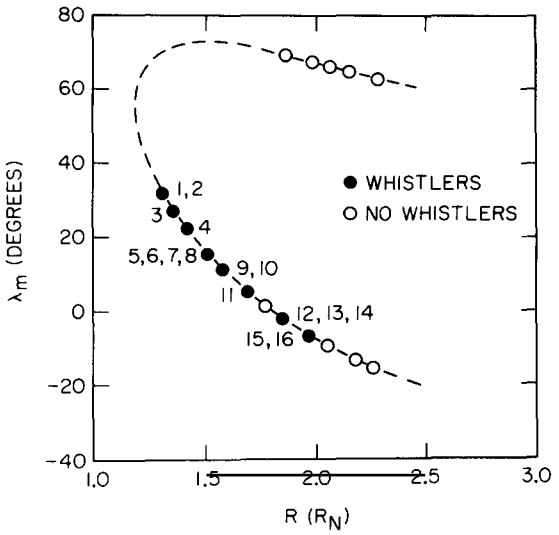

Fig. 6. The spacecraft trajectory near closest approach in radial distance and magnetic latitude coordinates. The black and open dots show the location of wideband frames with and without whistlers.

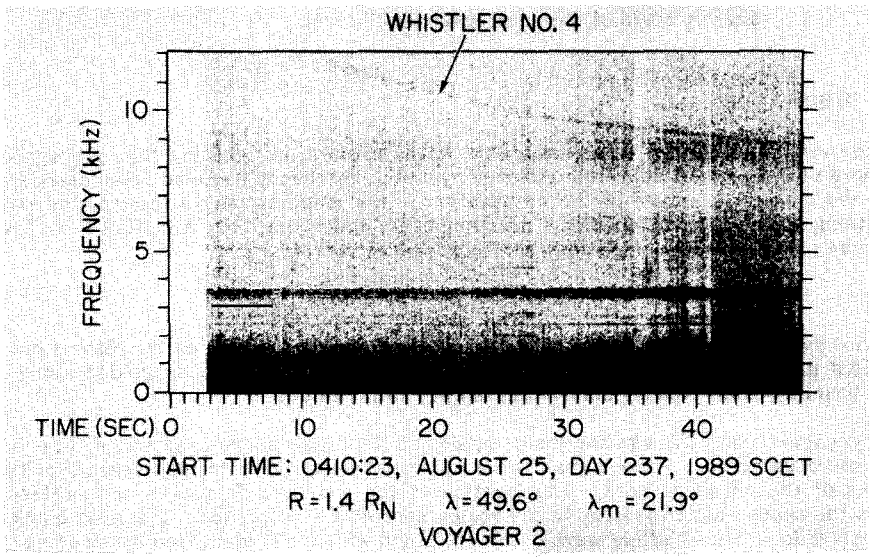

Fig. 7. A high resolution wideband spectrogram showing one of the sixteen whistlers detected in the region near closest approach. This is the best example of a whistler detected by Voyager during the Neptune flyby.

where c is the speed of light. The relatively high frequency of the whistlers, up to 12 kHz, indicates that the ray path must follow magnetic field lines that remain relatively close ($R < 3\ R_N$) to the planet. Otherwise the frequency would exceed the electron cyclotron frequency, and whistler mode propagation would not be possible. The electron density must also be relatively high, >10 cm^{-3}, at all points along the ray path. Otherwise significant deviations would be observed from the Eckersley law due to the close proximity of the wave frequency to the electron plasma frequency. The minimum electron density, ~10 cm^{-3}, implied by the whistler observations is substantially larger than the densities reported from the in situ plasma measurements /8/. Most likely the higher plasma densities are due to a cold component that cannot be detected by the Voyager plasma instrument.

Calculations of the dispersion using Equation 2 for various representative electron densities and magnetic field strengths shows that very long path lengths (50 to 4000 R_N) are required to explain the observed dispersion /5/. These long path lengths either imply much larger plasma densities than are indicated by

any of the presently available models or measurements, or a large number of bounces from one hemisphere to the other, or some combination of these effects. Large wave normal angles may also play a role. The most likely propagation paths probably involve multiple bounces through the dayside ionosphere, where existing models /17/ indicate relatively high densities (~10^5 cm^3). Even though the large dispersions strongly suggest that many bounces are involved, no evidence exists for a train of whistlers with steadily increasing dispersions. Whistler trains are commonly observed in the Earth's magnetosphere. The absence of whistler trains does not, however, rule out multiple bounces. It simply means that successive bounces cannot retrace the same ray path. Such propagation is entirely possible, and may be enhanced by certain special characteristics of Neptune's magnetic field configuration, such as the offset tilted dipole, and the presence of high order multiple fields near the planet. Detailed ray tracing analyses will be necessary to fully understand some of these effects.

PLASMA WAVE EMISSIONS IN THE INNER MAGNETOSPHERE

In addition to whistlers, several other types of plasma wave emissions were observed in the region near closest approach. All of these waves are very weak, less than ~100 μV/m. As can be seen in Figures 1 and 3 the dust impact noise is by far the most intense phenomena detected inside of 5 R_N. There is no evidence of intense whistler mode emissions (chorus and hiss), such as existed in the magnetospheres of Jupiter /18/, Saturn /19/, and Uranus /20/. The absence of intense whistler mode emissions is probably due to the low trapped radiation intensities in Neptune's magnetosphere /21/, compared to other planetary magnetospheres. It is also possible that the spacecraft did not pass through the proper region of the magnetosphere to detect intense waves associated with radiation belt particles. The very weak waves that do exist are in many cases difficult to interpret because of the uncertainty in the plasma density. Some of the waves that have been identified are indicated in Figure 3. These include a weak broadband background of whistler-mode noise at frequencies of about 20 kHz and below, z-mode emissions at frequencies slightly below the electron cyclotron frequency, and ion Bernstein waves /4/ at frequencies slightly above the proton cyclotron frequency. Relatively strong emissions also exist below the proton cyclotron frequency that could be due to either electrostatic or electromagnetic ion cyclotron waves /2/, although no detailed analysis has yet been performed. Another unusual phenomena is illustrated in Figure 8, which shows a mosaic of twelve 48-second wideband spectrograms obtained from 0405:33 to 0433:36 SCET, near the magnetic equator. In these spectrograms a closely bunched series of narrowband tones can be seen drifting slowly upward in frequency from about 3.3 to 3.8 kHz. Most likely these emissions are propagating in the whistler mode, since the frequency is between the electron and ion cyclotron frequency and below the electron plasma frequency (as deduced from the whistler analysis and the cutoff of the continuum radiation). The most puzzling feature of this noise is the fact that the frequency remains nearly constant even though the radial distance and magnetic latitude vary over a large range (1.3 to 2.3 R_N, and 33.0° to -17.3°). Since the magnetic field and plasma density probably vary significantly during this period, it is hard to understand how the emission frequency can remain so nearly constant. The understanding of these and other waves observed in the region near closest approach will require further study and investigation.

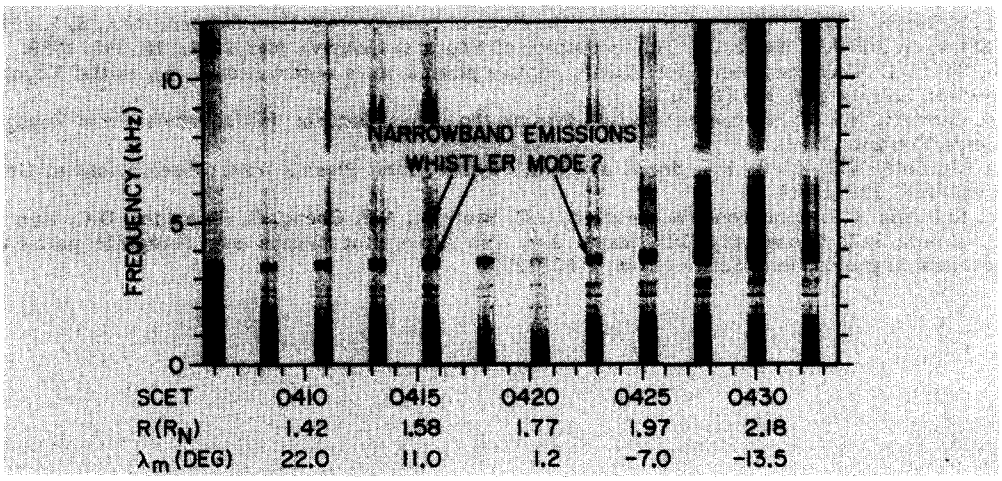

Fig. 8. A mosaic of twelve wideband frames obtained near the magnetic equator showing a series of narrowband emissions rising slowly in frequency from about 3.3 to 3.8 kHz. These emissions are unusual in that the frequency appears to be unaffected by changes in the local plasma parameter.

ACKNOWLEDGEMENTS

This research was supported by JPL contract 957723 with the Jet Propulsion Laboratory.

REFERENCES

1. F.L. Scarf and D.A. Gurnett, A plasma wave investigation for Voyager, *Space Sci. Rev.* **21**, 289 (1977).
2. D.A. Gurnett, W.S. Kurth, R.L. Poynter, L.J. Granroth, I.H. Cairns, W.M. Macek, S.L. Moses, F.V. Coroniti, C.F. Kennel, and D.D. Barbosa, First Plasma Wave Observations at Neptune, *Science* **246**, 1494 (1989).
3. W.S. Kurth, D.D. Barbosa, D.A. Gurnett, R.L. Poynter, and I.H. Cairns, Low Frequency Radio Emissions at Neptune, *Geophys. Res. Lett.* **17**, 1649 (1990).
4. D.D. Barbosa, W.S. Kurth, I.H. Cairns, D.A. Gurnett, and R.L. Poynter, Electrostatic Electron and Ion Cyclotron Harmonic Waves in Neptune's Magnetosphere, *Geophys. Res. Lett.* **17**, 1657 (1990).
5. D.A. Gurnett, W.S. Kurth, I.H. Cairns, and L.J. Granroth, Whistlers in Neptune's Magnetosphere: Evidence of Atmospheric Lightning, *J. Geophys. Res.*, in press (1990).
6. S.L. Moses, F.V. Coroniti, C.F. Kennel, W.S. Kurth, and D.A. Gurnett, Comparison of plasma wave measurements in the bow shocks at Earth, Jupiter, Saturn, Uranus, and Neptune, *Geophys. Res. Lett.* **17**, 1653 (1990).
7. N.F. Ness, M.H. Acuña, L.F. Burlaga, J.E.P. Connerney, R.P. Lepping, and F.M. Neubauer, Magnetic fields at Neptune, *Science* **246**, 1473 (1989).
8. J.W. Belcher, H.S. Bridge, F. Bagenal, B. Coppi, O. Divers, A. Eviatar, G.S. Gordon, Jr., A.J. Lazarus, R.L. McNutt, Jr., K.W. Ogilvie, J.D. Richardson, G.L. Siscoe, E.C. Sittler, Jr., J.T. Steinberg, J.D. Sullivan, A. Szaba, L. Villanueva, V.M. Vasyliunas, and M. Zhang, Plasma observations near Neptune: Initial Results from Voyager 2, *Science*, **246**, 1478 (1989).
9. J.W. Warwick, D.R. Evans, G.R. Peltzer, R.G. Peltzer, J.H. Romig, C. B. Sawyer, A.C. Riddle, A.E. Schweitzer, M.D. Desch, M.L. Kaiser, W.M. Farrell, T.D. Carr, I. dePater, D.H. Staelin, S. Gulkis, R.L. Poynter, A. Boischot, F. Genova, Y. LeBlanc, A. Lecacheux, Bent M. Pedersen, and P. Zarka, Voyager Planetary Radio Astronomy at Neptune, *Science* **246**, 1498 (1989).
10. D.A. Gurnett, The Earth as a radio source: The nonthermal continuum, *J. Geophys. Res.*, **80**, 2751 (1975).
11. D. Jones, Nonthermal continuum radiation at the radio planets, *Planetary Radio Emissions, Proc. of an International Workshop*, Graz, Austria, ed. by H.O. Rucker and S.J. Bauer, Austrian Acad. of Sci. Press, 11 (1985).
12. F.L. Scarf, D.A. Gurnett, W.S. Kurth, and R.L. Poynter, Voyager 2 plasma wave observations at Saturn, *Science* **215**, 587 (1982).
13. D.A.Gurnett, E. Grun, D. Gallagher, W.S. Kurth, and F.L. Scarf, Micron-sized particles detected near Saturn by the Voyager plasma wave instrument, *Icarus*, **53**, 236, 1983.
14. M.G. Aubier, N. Meyer-Vernet, and B.M. Pedersen, Shot noise from grain and particle impacts in Saturn's ring plane, *Geophys. Res. Lett.*, **10**, 5, 1983.
15. R. A. Helliwell, *Whistlers and Related Ionospheric Phenomena*, Stanford University Press, Stanford, CA, 1965.
16. T. L. Eckersly, 1929-1930 Developments in the study of radio propagation, *Marconi Rev.*, **5**, 1, 1931.
17. H. Shinagaw and J.H. Waite, Jr., The ionosphere of Neptune, *Geophys. Res. Lett.*, **16**, 945, 1989.
18. F.L. Scarf, D.A. Gurnett, and W.S. Kurth, Jupiter plasma wave observations: An initial Voyager 1 overview, *Science* **204**, 991 (1979).
19. D.A. Gurnett, W.S. Kurth, and F.L. Scarf, Plasma waves near Saturn: Initial results from Voyager 1, *Science* **212**, 235 (1981).
20. D.A. Gurnett, W.S. Kurth, F.L. Scarf, and R.L. Poynter, First Plasma Wave Observations at Uranus, *Science* **233**, 106 (1986).
21. S.M. Krimigis, T.P. Armstrong, W.I. Axford, C.O. Bostrom, A.F. Cheng, G. Gloeckler, D.C. Hamilton, E.P. Keath, L.J. Lanzerotti, B.H. Mauk, J.A. Van Allen, Hot plasma and energetic particles in Neptune's magnetosphere, *Science*, **246**, 1483, 1989.